Meas. Sci. Technol. **21** (2010) 025310 (7pp) doi:10.1088/0957-0233/21/2/025310

Whispering-gallery mode silica microsensors for cryogenic to room temperature measurement

Qiulin Ma, Tobias Rossmann and Zhixiong Guo[1]

Department of Mechanical and Aerospace Engineering, Rutgers, The State University of New Jersey, Piscataway, NJ 08854, USA

E-mail: guo@jove.rutgers.edu

Received 16 October 2009, in final form 4 December 2009
Published 19 January 2010
Online at stacks.iop.org/MST/21/025310

Abstract
Optical resonance shifts are measured against a wide range of temperatures from cryogenic to room temperature for silica microspheres operating at whispering-gallery modes. The sensor head microsphere is coupled to a fiber taper and placed in an insulated cell where the air temperature first cools down to below 110 K and then rises steadily and slowly. The transmission resonance spectrum of a distributed feedback laser at 1531 nm exciting the microsphere–taper system is monitored and recorded for every 1 K temperature increment. The resonance wavelength shifts against the temperature changes are analyzed. Several microspheres with size from 85 to 435 μm are tested. No significant dependence of the sensor sensitivity is seen with the sphere size. A cubic dependence of the wavelength shift versus the temperature is least-squares fitted. The measured sensitivity increases from 4.5 pm K^{-1} to 11 pm K^{-1} with increasing temperature in the test temperature range, and this behavior is consistent with the temperature dependence of the sum of thermal expansion and thermo-optic coefficients of silica material. The resolution of the sensors with the current instrument could reach 3 mK.

Keywords: cryogenic temperature, whispering-gallery mode, temperature microsensor, optical resonance shift, ultra-fine resolution

(Some figures in this article are in colour only in the electronic version)

1. Introduction

Optical whispering-gallery mode (WGM) phenomena in dielectric micro-resonators [1, 2] have been extensively studied over the past decade in many areas including cavity quantum electrodynamics [3], laser stabilization [4], micro-lasers [5], nonlinear optics [6] and miniature sensors [7–11]. Sensor applications which employ the interaction of the WGM evanescent component with an ambient analyte medium can be characterized into two categories: measurement of frequency/wavelength shifts of WGM resonance due to the change of effective refractive index and/or size of the resonator [7–12], and measurement of the amount of resonator's quality factor (Q) spoiling [13] or change of coupling efficiency [14, 15]. The state-of-the-art optical technology enables optical frequency measurement down to the level $\Delta f/f \sim 10^{-10}$, leading to the claim of extremely high sensitivity for nanoscale detection [8–10].

However, sensor material properties such as thermal expansion and the thermo-optic effect are susceptible to thermal fluctuations caused by either the ambient temperature variation or the absorption of laser energy during the laser scanning or optical pumping. These effects may induce appreciable resonance frequency/wavelength shifts, and thus, need to be considered in the development of resonance shift sensing techniques [7, 16]. Silica micro-bead temperature-induced resonance shift has been previously characterized in a narrow above-room-temperature range [7].

[1] Author to whom any correspondence should be addressed.

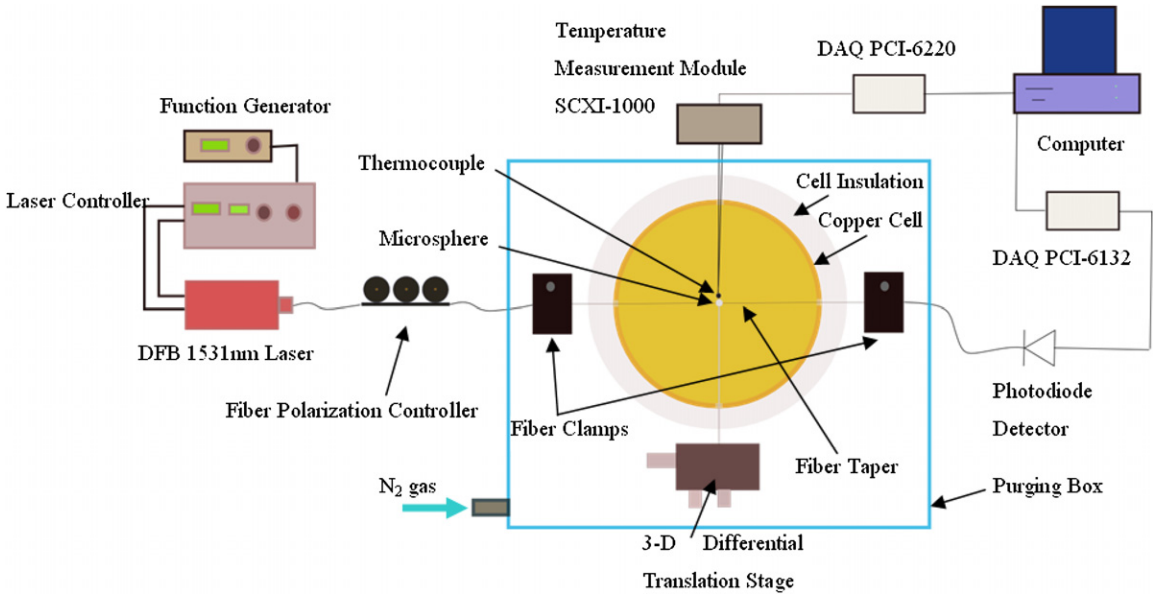

Figure 1. Schematic of the WGM sensing setup for cryogenic temperature measurement.

Here the investigation is extended to a broad temperature range. WGM-based temperature sensors have a potential use for cryogenic studies. There is a need for developing electromagnetic interference-immune high-resolution cryogenic temperature sensors. For example, in facilities using massive superconducting magnets, temperature data need to be recorded to actively control the magnet cool-down and warm-up, and to monitor the cryogenic system during operation. These systems often operate very close to their limits such that a rather small increase in temperature may cause a catastrophic failure. This requires good temperature stability, and therefore, fine resolution in its monitoring [17].

Cryogenic optical fiber sensors (COFS) operating at liquid nitrogen (LN_2) temperature level have been used to measure temperature conditions for superconductors. Lee *et al* [18] proposed a COFS with resolution ~0.4 K in the vicinity of room temperature and ~0.07 K in the vicinity of cryogenic temperatures using temperature-dependent emission characteristics of an erbium-doped fiber (EDF). Bertrand *et al* [19] realized an optical fiber temperature sensor based on the analysis of the decay time of the fluorescence emitted by special doped crystals bonded at the extremity of a multimode optical fiber, the excited state lifetime of which is greatly dependent on temperature. However, this kind of sensor is not cost-effective, and the resolution is limited by the fluorescence emission intensity and contrast of decay time in cryogenic temperatures. Ciotti *et al* [20] have studied a photo-imprinted Bragg grating fiber optic cryogenic temperature sensor. On illuminating the fiber with a broadband source of light, a narrow band is reflected by the grating at the Bragg wavelength. The resolution of the sensor of this type depends on two physical properties: the temperature dependence of the glass refractive index and its thermal expansion.

In this study, temperature measurements in a wide range from cryogenic to room temperature using the fiber WGM-based microsensor with an ultra-fine resolution are demonstrated. A thermally insulated optical test cell is designed. Realization of a cryogenic temperature environment for optical measurements via the use of a LN_2 container is discussed. A means for protection of frost formation on the optical system is introduced. Precise calibration of the laser tuning spectra is achieved by the use of a high-resolution optical spectrum analyzer. The WGM resonance spectra are recorded and the wavelength shifts are determined. The relationships of temperature versus wavelength shift are plotted for five microsensors. Finally, the measured temperature sensitivities are compared with the analytical values.

2. Experimental setup and methods

The experimental setup is sketched in figure 1. The WGM microsensor is made of a lab-fabricated silica microsphere [7] via fusing the tip of a silica single-mode bare fiber (Corning SMF-28) or fiber taper. The fiber taper used as a near-field coupler is also lab-fabricated by heating and pulling the same kind of single-mode bare fiber. The details of sphere and taper manufacturing and quality examination can be found in [7].

The fiber taper is aligned through two narrow slits of the optical test cell. The sensor head microsphere and a temperature-calibration thermocouple (Omega K-type with 0.01″ bead and 0.4 s time constant) are placed into the cell through another two slits of the optical test cell. The microsphere is precisely coupled with the fiber taper. The distributed feedback (DFB) laser (1531 nm) is tuned by a saw-shape injection current and launched into the optical fiber taper. The fiber passes through a polarization controller to optimize a TE mode coupling. The fiber modes couple more strongly to the TE modes than to the TM modes for microspheres [21].

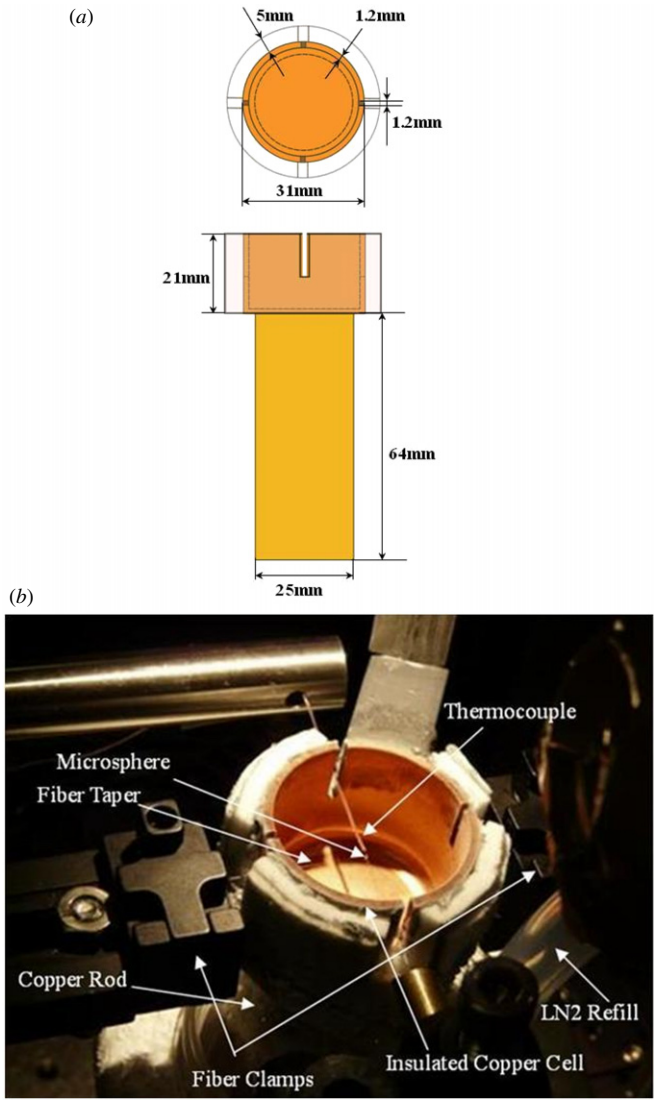

Figure 2. The sketch of the optical test cell: (*a*) top and side views of the cell with dimensions; (*b*) a photo of the cell showing structure and alignment.

The transmission signal is detected by a photodiode detector (Thorlabs PDA400) and recorded by a computer equipped with a high sampling rate data acquisition (DAQ) card (National Instrument PCI-6132) for acquiring WGM resonance spectra. The thermocouple is positioned about 0.1 mm away from the sensor head microsphere to measure the local air temperature. The signal from the thermocouple is acquired by a high-accuracy DAQ card (National Instrument PCI-6220) in the same computer.

The dimensions and a photo of the optical test cell are shown in figures 2(*a*) and (*b*), respectively. The cell is made of copper for efficient cooling. It is insulated with a layer of fiberglass to maintain cryogenic temperatures. The cell is 31 mm in diameter and 21 mm high. Four accessible slits with width 1.2 mm each are machined on four sides of the cell for placement of the fiber taper, thermocouple and microsphere, respectively. The open top of the cell is covered by a glass slide during experiment. This cover is partially wrapped with fiberglass, leaving a small window in the middle for viewing and optimizing the WGM coupling. After optimizing the WGM resonances, another glass slide wrapped with fiberglass is tightly attached onto the window with vacuum grease for further insulation.

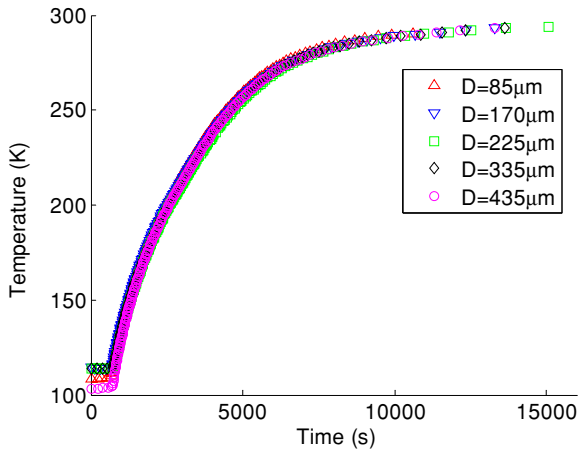

Figure 3. The measured air temperature changes in the optical test cell.

A solid copper rod is attached to bottom of the cell with silicone paste to ensure good thermal conductivity. An insulated LN_2 container is placed under the cell so that the copper rod is fully immersed into the liquid. Both the optical test cell and the container are placed inside a nitrogen purging box with a volume of 0.03 m^3. The box is purged for 30 min with a nitrogen flow rate 2000 cm^3 min^{-1} before injection of LN_2 into the container.

To cool down the air temperature in the cell, LN_2 is filled through a fiberglass-insulated tube into the container. Nitrogen purging continues during the entire experiment period to avoid frost formation on the optical system. The coldest air temperature achievable in the cell depends on the size of the LN_2 container, the LN_2 filling level, and the heat transfer between the cell and the container. The current experimental system can cool down the air temperature in the cell to roughly 100 K. For this study, stable temperatures in the range from 113 K to 293 K were experimentally achieved.

3. Results and discussion

Figure 3 shows the air temperature changes measured by the thermocouple in several tests with various microspheres placed into the optical test cell. It is seen that in the first few minutes, the air temperature remains at a stable low value and this value varies in different tests because it depends on the filling level of LN_2 in the container. Then the air temperature starts to increase slowly after the LN_2 level drops below the copper rod and steadily due to heat transfer with the external environment. The rate of temperature increase is a function of temperature; thus, it is seen that the spread of response when the temperature starts to increase is different for different tests. When the temperature is over 250 K, the difference of the spreads of temperature response between different tests

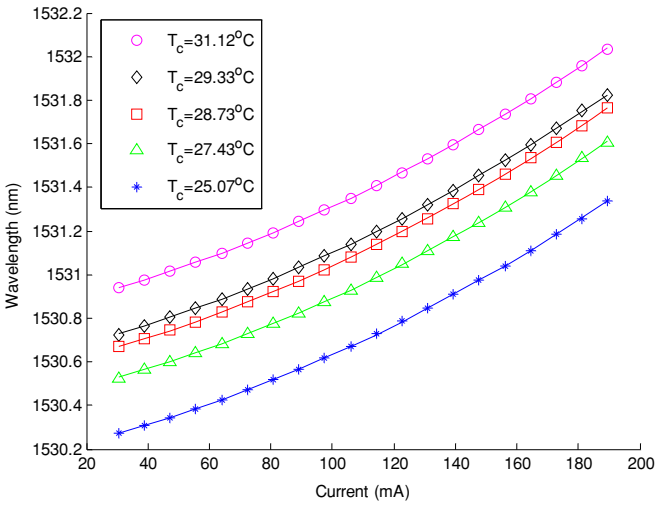

Figure 4. Calibration of the DFB1531 nm laser tuning at different controller temperatures.

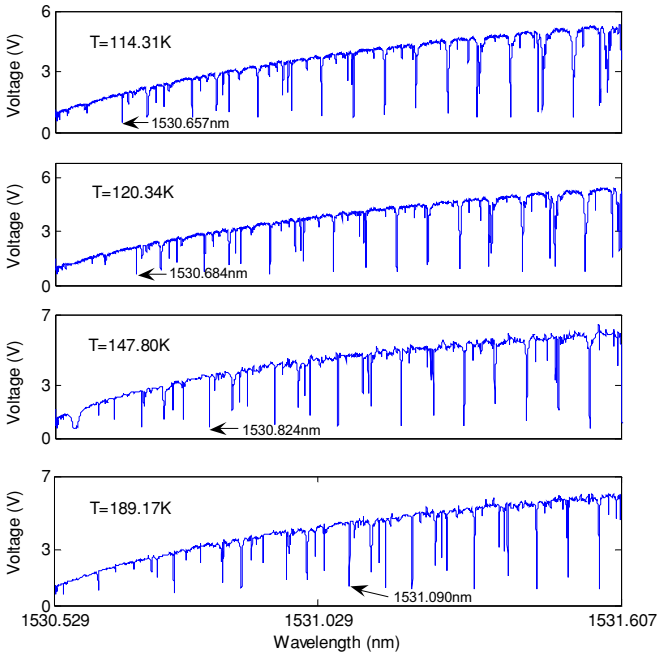

Figure 5. Typical transmission spectra of the microsphere 225 μm in diameter at four different temperatures.

is negligible. The initial rate of temperature increase is <0.1 K s^{-1}. It takes approximately 4 h to heat the cell from cryogenic temperature back to room temperature. The time constant of the thermocouple used for monitoring the temperature change is 0.4 s. The time constant for the silica microsphere depends on the sphere size, about 0.9 s for a sphere 450 μm in diameter and 0.03 s for a sphere 80 μm in diameter. Thus, the microspheres and the thermocouple are able to follow and reflect the air temperature variation in the cell.

Figure 4 shows five representative curves of the relationship between the lasing wavelength and the current in the laser diode controller for different controller temperatures. The laser tuning is calibrated by an optical spectrum analyzer (ANDO AQ6317B). Repeated testing has shown that the uncertainty is negligible, within $\pm$0.001 nm for each measurement point. The calibrated curves are utilized for accurately finding the resonance peaks in the WGM spectra. In the following temperature tests, the controller temperature T_c is selected such that the base resonance line is located close to the short-wavelength end in the wavelength tuning spectrum.

After optimizing the coupling with the 3D differential translation stage and the polarization controller, a significant WGM resonance that appears in each recorded spectrum is selected for measuring the resonance shift with respect to the temperature rise. Generally, the loaded Q value of the selected resonance is about 10^7 in the current study. Figure 5 shows the measured WGM spectra from a typical microsphere (225 μm) at four different temperatures. It should be noted that the spectra shown have been calibrated with the nonlinear laser tuning. Thus, the modes in figure 5 are linearly distributed in the wavelength abscissa.

Microspheres with diameter 85 μm, 170 μm, 225 μm, 335 μm and 435 μm, respectively, are measured for their wavelength shifts versus temperature change in the range from 113.7 $\pm$ 0.6 K to 292 $\pm$ 1.5 K, and the results are presented in figure 6. The two colors (blue and red in the online version) for each symbol represent shift values measured from two different WGM resonances with continuous temperature variation. This is because the tuning range of the laser is restricted to approximately 1 nm at a fixed controller temperature as shown in figure 4. However, the total optical shift of the WGM resonances in the wide temperature range could reach 1.4 nm, beyond this tuning range. It is worth mentioning that although two different WGMs are sampled, the shifts obtained from them overlap smoothly as shown in figure 6. The data can be well fitted by third-order polynomials. The coefficients of correlation for the five fitted curves are all above 0.999, and the 95% confidence intervals in the fittings are very small, usually within $\pm$0.20 pm, corresponding to a temperature uncertainty of 0.02 K.

Figure 7 plots the measured temperature sensitivities which are the slopes of the fitted curves in figure 6 for the tested microspheres. Although slight differences exist among the various size microspheres, no significant size effect is noted. The temperature sensitivity increases from 4.5 pm K^{-1} to 11 pm K^{-1} with increasing temperature in the test temperature range. It was noted that a linear laser tuning curve was assumed in the determination of the WGM shifts in [7]. From figure 4, such a linear assumption was inappropriate, and the sensitivities reported in [7] were inflated by approximately 20%. The corrected values are marked in figure 7, and they match with the tendency of the present measurement curves.

Through geometric optics and assuming linear thermal expansion and thermo-optic effects, the following analytical relationship for temperature tuning of the WGMs has been obtained [7]: $\mathrm{d}\lambda/\mathrm{d}T = (\alpha + \beta)\lambda$, where λ is the resonance wavelength in vacuum, T is the absolute temperature of the

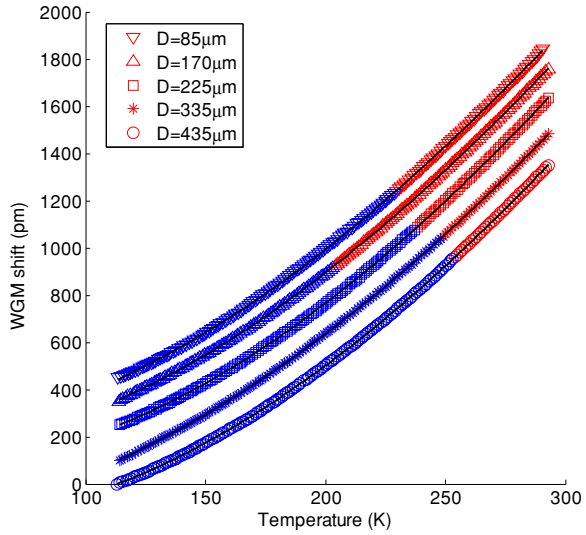

Figure 6. The measured data and least-squares cubic fitting curves of WGM resonance wavelength shift against temperature variation for five different microspheres. The shifts are raised by 100 pm, 250 pm, 350 pm and 450 pm for microspheres of 335 μm, 225 μm, 170 μm and 85 μm in diameter, respectively, for easier visualization.

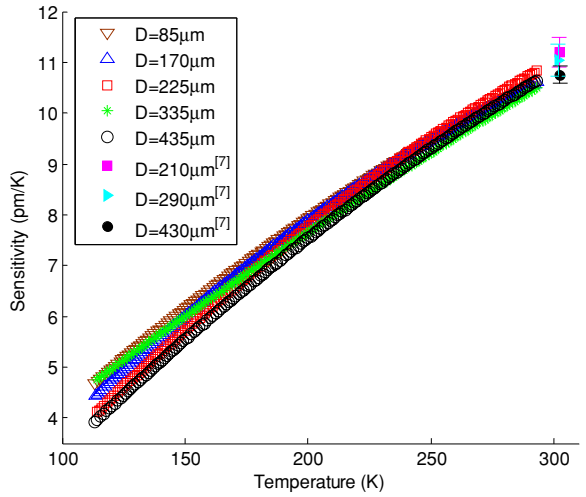

Figure 7. The measured temperature sensitivities of the five different microspheres and the corrected sensitivities for the cases studied in [7].

microsphere, α and β are the thermal expansion coefficient and thermal optic coefficient, respectively. These coefficients for fused silica from Corning SMF-28 fibers at wavelength 1531 nm are unknown. However, they are available in the literature for bulk Corning 7980 silica at wavelengths 1500 and 1600 nm [22, 23]. Generally, the thermal optic coefficient of Corning 7980 silica is much larger than the thermal expansion coefficient.

Figure 8 compares the measured sensitivity averaged from the five test microspheres with the analytical sensitivity calculated based on the material properties of bulk Corning 7980 silica. The measured sensitivity can be expressed by a

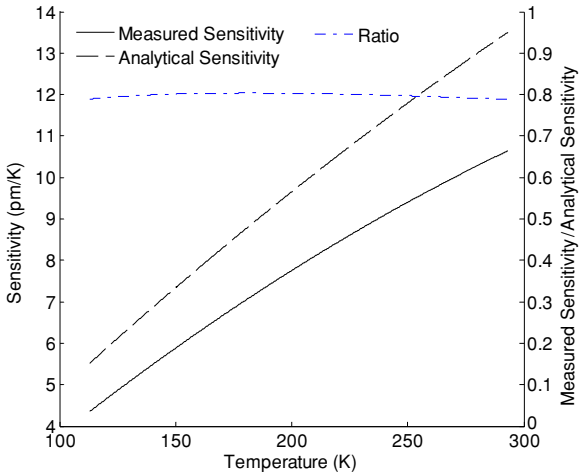

Figure 8. Comparison of the measured sensitivity with the analytical sensitivity based on the properties of bulk Corning 7980 silica, and the ratio profile of the measured sensitivity to the analytical value in the test temperature range.

quadratic equation

$$d\lambda/dT = -(4.48 \pm 0.30) \times 10^{-5}T^2 + (5.31 \pm 0.12) \times 10^{-2}T - (1.08 \pm 0.12). \quad (1)$$

The uncertainties in the three coefficients of the equation give 95% confidence intervals. The analytical sensitivity curve can also be fitted by a quadratic relationship. Thus, the cubic fittings in figure 6 are reasonable. From figure 8, it is observed that the varying pattern of the experimental sensitivity curve is similar to the analytical one. The profile of the ratio of the experimental sensitivity to the analytical sensitivity against the temperature is also plotted in figure 8. It is seen that this ratio profile is nearly linear, varying in a narrow range between 0.79 and 0.80. It may indicate that the sum of $(\alpha + \beta)$ for the fused silica microspheres made of the Corning SMF-28 fiber is approximately 79–80% of the value for bulk Corning 7980 silica.

The temperature resolution of a WGM sensor is formulated as [7]

$$\Delta T_{\min} = \Delta\lambda_{\min}/(d\lambda/dT), \quad (2)$$

in which $\Delta\lambda_{\min}$ is the wavelength resolution of the instrument and $d\lambda/dT$ is the temperature sensitivity of the microsphere. The wavelength resolution is restricted by the linewidth of the scanning laser, the sampling rate in data acquisition, and the loaded WGM resonance Q factor. Suppose the wavelength tuning range of a scanning laser is $\Delta\lambda$ (~0.01–1 nm), the tuning frequency of the laser is f_s (~1–10 Hz), and the DAQ card has a sampling rate S, then the minimum tuning wavelength is $\Delta\lambda f_s/S$. Since the sampling rate can go up to dozens of GHz, data sampling is usually not a limiting factor for the wavelength resolution. As for the Q factor, the minimum resolvable resonance shift is about one-hundredth of the resonance linewidth $(\lambda/(100Q))$ [24]. Since the intrinsic Q-value of a microsphere resonator is extremely high, the loaded Q can always push to the limit of the laser linewidth. Therefore, Q-value may not be a limiting factor. In the current

instrument, $\Delta\lambda_{min}$ is limited by the laser linewidth. The current DFB laser has a linewidth of 2 MHz, equivalent to 0.0156 pm. From sensitivity equation (1), $d\lambda/dT$ is obtained as 10.82 and 5.877 pm K^{-1} for temperature at 300 K and 150 K, respectively. Thus, the minimum resolvable temperature of the current instrument is 1.4 mK and 2.7 mK for temperature at 300 K and 150 K, respectively. No existing cryogenic temperature measurement devices exhibit such a high resolution.

The optical fiber temperature sensor usually has a resolution of 0.3 K in the temperature range of 20–120 K [19]. Ciotti *et al* [20] claimed a temperature measurement resolution of 0.02 K. However, its sensor response time is slow, on the order of 1 s. The WGM sensor has a quick response. For instance, the time constant of a silica microsphere 80 μm in diameter is only 0.03 s. As an optical fiber sensor, the WGM sensor can be certainly applied to a cryogenic temperature range on the order of 10 K, although the current infrastructure cannot realize such a low temperature. At 50 K, the sensor sensitivity analytically evaluated from the values of thermal expansion and optical coefficients [22, 23] is 1.301 pm K^{-1}, giving a temperature resolution of 0.012 K. The state-of-the-art laser technology has pushed the laser linewidth to a few kHz, i.e. almost three orders of magnitude reduction as compared with the DFB laser used in the current instrument. In such a case, it is possible to reduce the WGM sensor temperature resolution by three orders of magnitude, i.e. to the level of 10^{-6} K.

4. Conclusion

Silica microsphere–taper coupled optical WGM microsensors are tested for cryogenic to room temperature measurement. The optical test cell is designed to ensure a slow and stable temperature variation at cryogenic temperatures. Nitrogen purging is utilized to prevent frost formation on the optical system. All the test sensors show an excellent third-order polynomial dependence of the resonance wavelength shift on the temperature change. The shape of the measured sensitivity curve follows the analytical variation very well, except that the values of the measured sensitivity are generally 79–80% of the analytical values. This difference may be attributed to the material properties used in the analysis. The silica microspheres used in the experiments are fused with the Corning SMF-28 fiber whose thermo-optical properties are unknown, while the thermal expansion and thermo-optic coefficients used in the analysis are based on data for bulk Corning 7980 silica in the literature. In the cryogenic temperature range, it is found that the sensitivity has no significant size dependence for the test microspheres. The measured sensitivity increases from 4.5 pm K^{-1} to 11 pm K^{-1} with increasing temperature in the test temperature range. The resolution of the current sensors and instrument could reach 3 mK at cryogenic temperatures. The demonstration of the WGM sensor feasibility in cryogenic temperature measurement with ultra-fine resolution enables its potential applications interfacing with electro-optical devices and cryogenic systems.

Acknowledgments

Z Guo acknowledges partial support to the work by the National Science Foundation under grant no CBET-0651737 and by US Department of Agriculture under CSREES Award 2008-01336.

References

[1] Gorodetsky M, Savchenkov A and Ilchenko V 1996 Ultimate *Q* of optical microsphere resonators *Opt. Lett.* **21** 453–5
[2] Sandoghdar V, Treussart F, Hare J, Lefevre-Seguin V, Raimond J and Haroche S 1996 Very low threshold whispering-gallery-mode microsphere laser *Phys. Rev.* A **54** R1777–80
[3] Vernooy D, Furusawa A, Georgiades N, Ilchenko V and Kimble H 1998 Cavity QED with high-*Q* whispering-gallery modes *Phys. Rev.* A **57** R2293–6
[4] Vassiliev V, Velichansky V, Ilchenko V, Gorodetsky M, Hollberg L and Yarovitsky A 1998 Narrow-line-width diode laser with a high-*Q* microsphere resonator *Opt. Commun.* **158** 305–12
[5] Cai M, Painter O, Vahala K and Sercel P 2000 Fiber-coupled microsphere laser *Opt. Lett.* **25** 1430–2
[6] Braunstein D, Khazanov A, Koganov G and Shuker R 1996 Lowering of threshold conditions for nonlinear effects in a microsphere *Phys. Rev.* A **53** 3565–72
[7] Ma Q, Rossmann T and Guo Z 2008 Temperature sensitivity of silica micro-resonators *J. Phys. D: Appl. Phys.* **41** 245111
[8] Arnold S, Khoshsima M, Teraoka I, Holler S and Vollmer F 2003 Shift of whispering-gallery modes in microspheres by protein adsorption *Opt. Lett.* **28** 272–4
[9] Quan H and Guo Z 2005 Simulation of whispering-gallery-mode resonance shifts for optical miniature biosensors *J. Quant. Spectrosc. Radiat. Transfer* **93** 231–43
[10] Quan H and Guo Z 2007 Simulation of single transparent molecule interaction with an optical microcavity *Nanotechnology* **18** 375702
[11] Nguyen N Q and Gupta N 2009 Analysis of an encapsulated whispering gallery mode micro-optical sensor *Appl. Phys.* B **96** 793–801
[12] White I M, Oveys H and Fan X D 2006 Liquid-core optical ring-resonator sensors *Opt. Lett.* **31** 1319–21
[13] Armani A and Vahala K 2006 Heavy water detection using ultra-high-*Q* microcavities *Opt. Lett.* **31** 1896–8
[14] Laine J, Tapalian H, Little B and Haus H 2001 Acceleration sensor based on high-*Q* optical microsphere resonator and pedestal antiresonant reflecting waveguide coupler *Sensors Actuators* A **93** 1–7
[15] Guo Z, Quan H and Pau S 2006 Near-field gap effects on small microcavity whispering-gallery mode resonators *J. Phys. D: Appl. Phys.* **39** 5133–6
[16] Dong C, He L, Xiao Y, Gaddam V, Ozdemir S, Han Z, Guo G and Yang L 2009 Fabrication of high-*Q* polydimethylsiloxane optical microspheres for thermal sensing *Appl. Phys. Lett.* **94** 231119
[17] Lefevre P and Petterson T 1995 The large hadron collider—conceptual design *CERN Report* No. CERN/AC/95–05 (LHC)
[18] Lee Y and Lee B 2002 High resolution cryogenic optical fiber sensor system using erbium-doped fiber *Sensors Actuators* A **96** 25–7
[19] Bertrand S, Jalocha A, Tribillon G, Bouazaoui M and Rouhet J 1996 Optical fibre temperature sensor in the cryogenic range *Opt. Laser Technol.* **28** 363–6

[20] Ciotti M, Nardelli V, Caponero M A, Felli F, Lupi C and Ippoliti L 2007 An optical system for cryogenic temperature measurements *Smart Mater. Struct.* **16** 1708–11

[21] Humphrey M, Dale E, Rosenberger A and Bandy D 2007 Calculation of optimal fiber radius and whispering-gallery mode spectra for a fiber-coupled microsphere *Opt. Commun.* **271** 124–31

[22] Leviton D and Frey B 2006 Temperature-dependent absolute refractive index measurements of synthetic fused silica *Proc. SPIE* **6273** 62732K

[23] Barron T and White G 1999 *Heat Capacity and Thermal Expansion at Low Temperatures* (New York: Plenum) p 307

[24] Vollmer F and Arnold S 2008 Whispering-gallery-mode biosensing: label-free detection down to single molecules *Nature Methods* **5** 591–6